INTERFACE

royalsocietypublishing.org/journal/rsif

Research

Cite this article: Avinery R, Aina KO, Dyson CJ, Kuan H-S, Betterton MD, Goodisman MAD, Goldman DI. 2023 Agitated ants: regulation and self-organization of incipient nest excavation via collisional cues. *J. R. Soc. Interface* **20**: 20220597.
https://doi.org/10.1098/rsif.2022.0597

Received: 16 August 2022
Accepted: 24 April 2023

Subject Category:
Life Sciences–Physics interface

Subject Areas:
biophysics, computational biology

Keywords:
fire ants, cellular automata, excavation dynamics, behavioural model

Author for correspondence:
Daniel I. Goldman
e-mail: daniel.goldman@physics.gatech.edu

Agitated ants: regulation and self-organization of incipient nest excavation via collisional cues

Ram Avinery[1], Kehinde O. Aina[2], Carl J. Dyson[3], Hui-Shun Kuan[4], Meredith D. Betterton[4], Michael A. D. Goodisman[3] and Daniel I. Goldman[1]

[1]School of Physics, [2]Institute for Robotics and Intelligent Machines, and [3]School of Biological Sciences, Georgia Institute of Technology, Atlanta, GA, USA
[4]Department of Physics, University of Colorado Boulder, Boulder, CO, USA

RA, 0000-0002-9580-4989; H-SK, 0000-0003-2604-6448; MDB, 0000-0002-5430-5518; MADG, 0000-0002-4842-3956

Ants are millimetres in scale yet collectively create metre-scale nests in diverse substrates. To discover principles by which ant collectives self-organize to excavate crowded, narrow tunnels, we studied incipient excavation in small groups of fire ants in quasi-two-dimensional arenas. Excavation rates displayed three stages: initially excavation occurred at a constant rate, followed by a rapid decay, and finally a slower decay scaling in time as $t^{-1/2}$. We used a cellular automata model to understand such scaling and motivate how rate modulation emerges without global control. In the model, ants estimated their collision frequency with other ants, but otherwise did not communicate. To capture early excavation rates, we introduced the concept of 'agitation'—a tendency of individuals to avoid rest if collisions are frequent. The model reproduced the observed multi-stage excavation dynamics; analysis revealed how parameters affected features of multi-stage progression. Moreover, a scaling argument without ant–ant interactions captures tunnel growth power-law at long times. Our study demonstrates how individual ants may use local collisional cues to achieve functional global self-organization. Such contact-based decisions could be leveraged by other living and non-living collectives to perform tasks in confined and crowded environments.

1. Introduction

A variety of complex systems display collective behaviours [1–4]. These collective activities often originate through the process of self-organization [1,5,6]. Self-organization represents a remarkable phenomenon whereby individuals engage in relatively simple interactions leading to sophisticated, collective actions [2,7,8]. The emergence of collective behaviours through self-organization represents an important phenomenon across physical and biological systems and scales [1–3].

Highly social animals are key systems for studying collective behaviours. For example, highly social insects, which include all ants and termites, as well as some bees, wasps, thrips, beetles and aphids, are remarkable in their ability to coordinate activities and self-organize to behave as a single 'superorganism' [9–11]. The tremendous success of many social insects relies critically on the collective actions that lead to nest construction [10–19]. Nests provide protection and hospitable environments for rearing offspring [20,21]. Nests may also contain networks of tunnels and chambers used to house individuals and food [19,22–30]. In general, the social insect nest represents a fundamental part of the extended phenotype of the society [16].

The behaviours leading to the successful construction of nests by social insects are remarkable [7,12,31–36]. No single individual has a conception of how the nest should be built or what it should look like when completed

THE ROYAL SOCIETY PUBLISHING

[34,37]. Instead, social insects self-organize by using behavioural rules that lead to the formation of complex structures [1,3,5,34,38,39]. Higher-level nest patterns emerge from simple, lower-level interactions and environmental cues [3,7,31,34,35,39–41]. The evolutionary success of insect superorganisms such as an ant colony relies on adaptive regulation to manage competing priorities including safety, rest, hunger and reproduction [42,43]. Uncovering the mechanisms of coordination underlying such regulation is key to understanding social behaviour and serves as inspiration for protocols to be implemented in synthetic collectives.

A major goal of the study of collective behaviour is to understand the rules governing group activities. For example, during fresh nest excavation, it may seem straightforward that ants which cannot find existing tunnels would choose to dig new ones; however, it is not as obvious how ants collectively deprioritize excavation when a system of tunnels is sufficiently developed. Early nest excavation in ants and termites displays consistent rate regulation [44–46]. This has previously been attributed to a recruitment process and modelled using a logistic model, without mechanistic explanation [44]. More recently, Bruce *et al*. [45] suggested that ants regulate excavation rate through encounters in a manner that is collective-size dependent and sensitive to existing tunnels for small collectives. The excavated area over time was concluded to follow a Michaelis–Menten curve [47], suggestive of a self-inhibiting mechanism whereby the existence of excavated area inhibits further excavation. Bruce *et al*. interpreted their results as an indication that the ants attempted to minimize contact with each other; however, few studies have directly provided a window into the individual decision making and how it affects an emergent collective outcome.

Interactions between individuals could occur through a variety of communication mechanisms including chemicals, sound and contact. Underground and in the absence of light sources, vision is unlikely to contribute to individual interactions, as evidenced by the evolved blindness of termite soldiers [48]. Instead, chemicals, such as pheromones, are often cited as the dominant mode of communication for collective task regulation [48,49]. However, the proximate mechanisms used to convey information across biological collectives remain poorly understood.

The goal of this investigation was to gain a greater understanding of the dynamics underlying the successful excavation of nests in biological collectives. We wished to understand the proximate biological and physical mechanisms that ants use to regulate nest excavation, and to determine how various individual and group behaviours affect the overall dynamics. Our interest was specifically to determine if excavation regulation could emerge from independent individual decisions without invoking communication through chemical, visual or acoustic signals. Inspired by our recent studies on contact-responsive robotic collectives [50,51], we explored how contact sensing, as an information source, may contribute to global excavation regulation without other communication. To discover a minimal model, we make a simplifying assumption that ants make decisions based on their recent experiences, where encounters with others are registered but no information is actively passed between them. Our research makes use of experiments of ant excavation and subsequent mathematical modelling and computer simulation used to interpret the experimental results. Our models exhibit remarkable agreement with the experiments, suggesting that collectives can successfully rely on simple contacts to coordinate their group activities, and Further, our model can generate testable predictions for further experimental studies.

2. Methods

2.1. Ant excavation experiment

We investigated substrate excavation dynamics in small groups of the fire ant *Solenopsis invicta* [52]. *Solenopsis invicta* ants are master builders. They successfully construct complex nests in soils or granular substrates found around the world using a diversity of materials [14,46,48,52–54]. The *S. invicta* nest is a complex, sophisticated structure that allows individuals to move and rear offspring. The nest is fundamentally important to the success of *S. invicta* colonies and is one of the most conspicuous features of this social insect.

Three colonies of *S. invicta* were collected from Atlanta, Georgia, USA during the fall of 2020. Individuals were separated from soil using the drip flotation method [55]. Collected individuals were then housed in plastic containers and supplied with water and food as needed to ensure their continued survival.

We sought to visualize the behaviours that *S. invicta* workers engaged in while excavating tunnels, to gain a greater understanding of the processes they use to construct nests. To do so, we monitored ant substrate excavation dynamics in experimentally created arenas, over many hours. Experiments were conducted inside set-up consisting of two areas accessible by the fire ants: an open entrance area to which ants were added for each trial and a digging area connected by a tunnel where excavation behaviours could be monitored through an acrylic wall (figure 1). The excavation arena consisted of a $195 \times 145 \times 2.5$ mm^3 quasi-two-dimensional space, defined by a three-dimensional-printed frame, to allow for monitoring of tunnel growth and ant activity. Glass particles measuring 0.7 ± 0.1 mm in diameter were used as an artificial substrate to be manipulated by the ants. Moisture content of the substrate was maintained at 10% water by weight across all trials; we have previously shown that *S. invicta* ants' excavation rate is insensitive to moisture content in the range of 5–20% [56]. The walls of the arena and entrance area were coated with talcum powder to ensure that ants could not climb out of the designated spaces. During experimental excavation trials, a controlled number of ants were transferred manually from the collected colony to the digging arena. Non-warming LED light sources were directed at the digging area to offer illumination for recording.

We allowed groups of *S. invicta* workers to excavate within the artificial arenas. For each trial, groups of 40–70 randomly selected worker fire ants were transferred into the apparatus. In total, nine experimental trials were included in this study, using ants from three colonies, each used in at least two trials. Recording was started immediately following the addition of ants to the entrance area of the experimental set-up. Once introduced into the entrance, the ants were allowed to migrate independently down into the digging arena. Fire ant excavation in the digging arena was monitored and recorded for up to 70 h in each trial, which was recorded at 24 frames per second (fps) using a consumer computer camera (Logitech C920), at a resolution of 1920×1080 pixels.

2.2. Video analysis

To elucidate behavioural patterns involved in nest construction, we quantified collective excavation, ant spatial distribution, tunnel morphology, as well as individual ant–ant interactions, through manual and automated video tracking.

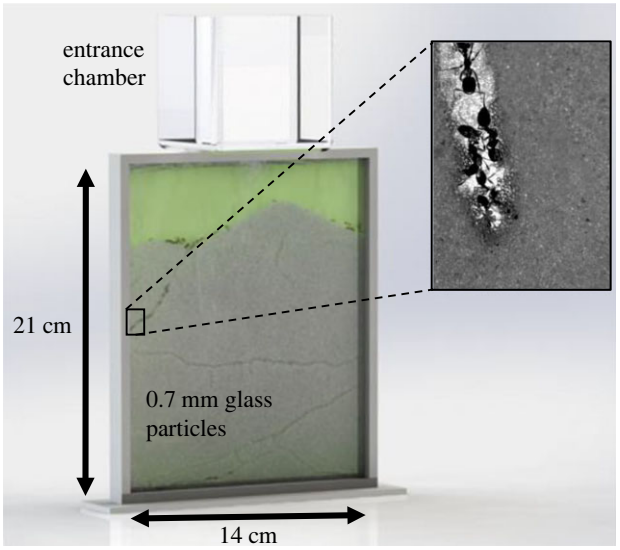

Figure 1. Experimental set-up—three-dimensional rendering. A custom-made plastic frame holds acrylic sheets 2.5 mm apart. The accessible part of the system is 14 cm wide and 21 cm tall. Approximately two-thirds of the volume is filled with a substrate—0.7 mm glass particles with the moisture content adjusted to 10% by weight. A top container serves as an entrance chamber where 40–70 ants are placed to start the experiment. The experimental trials are recorded using a commercial webcam.

To estimate ant participation in excavation, we used captured colour differences to classify image pixels belonging to ants, as well as to detect the substrate interface. We used a bright green sheet as the background for the digging arena, which produced a visual contrast with the substrate, as well as with the ants; this contrast made for convenient video analysis based on colour differences (figure 2*a*,*b*).

Within our experiments, we defined ants as participating in some aspect of the excavation process if they were below the substrate interface. Once pixels were classified as belonging to ants below the substrate interface, the pixel count was converted to an estimate of the number of ants, using a calibration curve from a linear fit of manually counted ants versus detected pixel count, tabulated over multiple time points, for each recorded video.

We were interested in observing the excavation progression and rate regulation by detecting the excavated tunnels over time. This was done by following areas in the digging arena newly explored by the ants. Procedurally, we could accumulate a map of pixels that were classified as belonging to an ant at any given time in the past. However, the small amount of noise inherent in that technique, when accumulated, produces too many spurious detections of newly explored areas. Instead, we found that calculating and accumulating motion detection produced much less noise. To calculate motion detection, we down-sampled our videos in time to 12 fps by averaging subsequent frames, and then calculated the difference between the resulting frames. The result was then subjected to Gaussian filtering and a threshold was applied. The threshold was determined dynamically as five times the standard deviation of the Gaussian filtered values, over a region of the video determined to not have been excavated throughout the recording (manually). Figure 2*c* shows an example of motion-detected pixels, red (blue) indicates pixels that became lighter (darker) between successive down-sampled frames. A map of accumulated motion-detected pixels was recorded over each recorded trial.

Ants occasionally reversed and backed out of a tunnel when their path was blocked by other ants. Reversal is an important behaviour that minimizes traffic clusters [57] and we wanted to observe its relation to the number of ants in the tunnels and the overall excavation rate. We, therefore, tabulated event

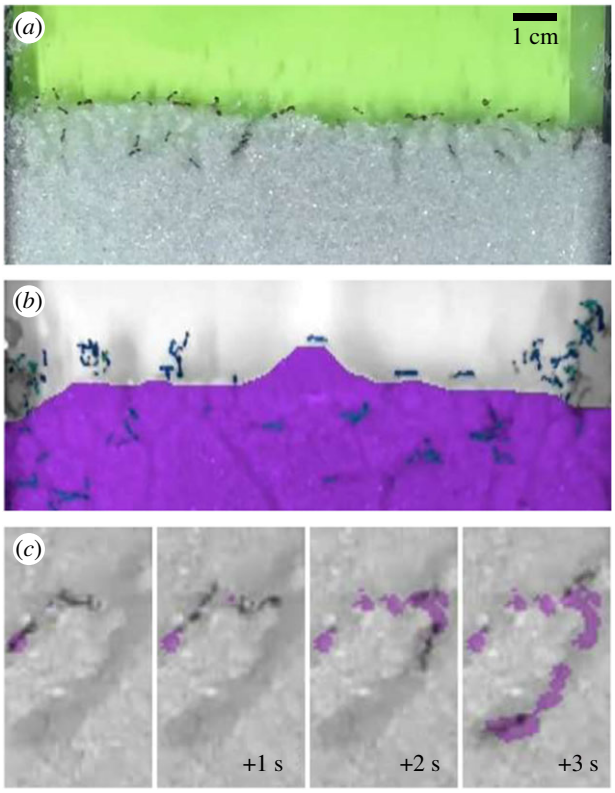

Figure 2. Experimental recording and tracking. Each trial was recorded at 24 frames per second using a commercial webcam. (*a*) The digging arena is enclosed between acrylic sheets and composed of glass beads. A green background is used to generate suitable contrast between the substrate and excavated tunnels. Image 40 min after the introduction of ants into the apparatus is shown. (*b*) The colour difference between ants, substrate and background allows for substrate tracking (shaded purple) as well as ant tracking (shaded blue). Together, the number of pixels associated with ants below the substrate is used to quantify the participation in the excavation activity. (*c*) Motion detection of ants was found to be a robust method to track the exploration of the system, and thereby allowed us to quantify the excavated area over time. We calculate the difference between each pair of sequential frames, apply a threshold and accumulate the result over time (purple shade). See Methods for additional details.

counts of ants reversing without excavating a bolus of substrate material, following an encounter with another ant. This was done for several non-branching tunnels, in multiple experiments, by visual inspection.

2.3. Cellular automata model

To gain an understanding of the ant excavation dynamics, particularly in the earlier times of excavation, we employed a cellular automata (CA) model adapted from that in our previous work [57]. A CA model allows us to focus on the behavioural aspect, without a need to implement detailed mechanics of walking and digging. The simulation process boils down to a small set of time-evolution and interaction rules that are applied at every discrete step. Using this model, we may conveniently test various behavioural rules and then test how the CA model's emergent collective behaviour matches experimental observations.

In the simulated system, ants walk through a linear tunnel that is composed of discrete cells that accommodate two ants each, going in either the same or opposite directions (figure 3). A tunnel has an entry into a sequence of 'substrate-free' cells, followed by cells filled with substrate. At each time step (TS), ants move along the tunnel until they reach substrate; at which point they pause and excavate pellets. Once a substrate cell is drained

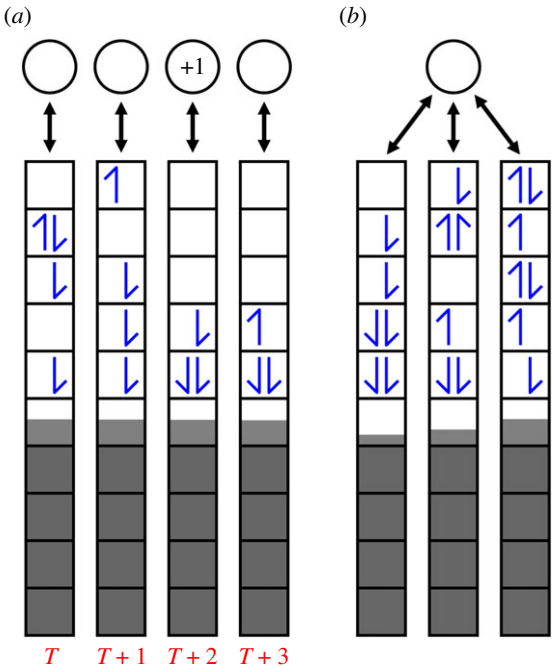

Figure 3. Cellular-automata simulation of ant excavation. Within this model, ants from the outside reservoir (circle on top) randomly decide to enter the system, with a probability determined by each individual. Once inside, the ants (blue half-arrows) move along a tunnel composed of discrete cells. Each cell accommodates up to two ants. An ant moves from the entrance (top) towards the substrate (bottom, in grey), but cannot move into the substrate. Once an ant reaches the first substrate cell, it removes (i.e. excavates) pellets from it, one every time step. After reaching its pellet holding capacity, an ant reverses and moves back towards the entrance to deposit the excavated pellets. Substrate cells are initialized to contain a consistent number of pellets, which are then depleted by the incoming ants. The number of pellets remaining in the first reachable substrate cell is indicated by the degree of filling of lighter grey. (*a*) Four consecutive time steps, showing four ants in a single tunnel, at first (time T) with one heading out towards the entrance, two on their way towards the substrate and one already at the substrate interface. At $T + 1$, another ant reaches the substrate, and the third is a cell behind. Since the next cell is occupied by two ants, the latter ant, at time $T + 2$, decides to reverse and head back towards the entrance without excavating. Also at $T + 2$, an ant steps outside and increases the count of ants in the outside reservoir (number in circle). The ants at the interface remain there to excavate until either the cell is depleted or their individual capacity is full. (*b*) In a multi-tunnel model, ants from the outside reservoir randomly decide to enter, as before, and also randomly uniformly choose which tunnel to go into. Once inside, the dynamics are as in a single independent tunnel.

of its pellets, it becomes available for ants to walk into. In this way, the tip of the tunnel, where the substrate starts, elongates over time.

Within this computational model, a cell represents a single ant body-length's (BL) worth of tunnel. Tunnels made by *S. invicta* generally converge to approximately two ant body-widths (BW) [46] and allow most ants to pass each other unhindered. We, therefore, take cells to represent an area of BL × BW and allow two ants to occupy each. At each TS, an ant will move to the next cell, if it is empty, and will thereby be moving at a speed of BL/TS. By quantifying the typical ant speed within tunnels, we relate the simulation timescale to the excavation experiment timescale. Within the simulation, we parametrize the number of pellets in a cell full of the substrate and the number of pellets an ant will excavate each time; these, respectively, represent the typical accumulated time it takes the ants to excavate a BL length of the tunnel, and the typical time spent at the tunnel tip by each ant.

As mentioned above, two ants may occupy the same cell and pass each other unhindered under this model. Three (or more) body collisions occur when an ant tries to move into a cell that is already occupied by two other ants. In response to such a collision, an ant that is heading towards the tip of the tunnel randomly chooses whether to reverse course without digging, with a predetermined probability. We find that our results are not sensitive to this reversal probability within the range (0.1, 0.9), and choose to fix this value to 0.34, as previously used [57]. An ant that is headed towards the exit never relents. In our previous work, we used only a single simulated tunnel [57], but here we use multiple tunnels to capture the observed experimental behaviour, as discussed below. Within the multi-tunnel CA model, when ants enter a tunnel, they first randomly and uniformly choose which of the multiple tunnels to go into. From there, the simulation proceeds as previously discussed.

2.4. Ant speed measurements

We analysed image maps to estimate an ant's walking speed within tunnels. Given tracked exploration maps (figure 4), we extracted an example of a long branch-less tunnel and generated a linearized profile through the following steps: (i) fit a centre-line spline, (ii) generate perpendicular cross-sections at equal longitudinal intervals (figure 5*a*), and (iii) sum binarized pixel values across each cross-section. As ants walk through the tunnel, the linearized profile displays a travelling cluster of high values. We lay out these linear profiles over time as a space–time diagram (figure 5*b*,*c*). We then use a sliding time window of 1 min and for each window run a line-detection algorithm (figure 5). Ant walking speeds are captured as the detected line slopes. We accumulated the distribution of observed speeds for well-detected lines. Through thousands of detected slopes, we observed a mean speed of 0.27 ± 0.09 BL s^{-1}.

2.5. Model fitting

To fit the experimentally observed excavation rate, we iterated through randomly generated values for the free parameters of the simulated model and compared with the observed curves. Other fixed parameters have been determined either in previous work or in this study (table 1). The CA simulation time has been rescaled such that the ant nominal speed BL/TS is the experimentally determined mean ant walking speed. The model we fit then has four free parameters—number of tunnels, work–rest imbalance constant (τ_0), relaxation length (L_0) and steady-state participation level (we discuss the meaning of these parameters in Section 3).

We started by generating 10 000 uniformly random sampled sets of parameters, in a wide range. To test a fit over multiple timescales, we first converted both the observed curve and each simulation curve to log-rate over log-time, by averaging within exponentially spaced bins and then taking the log of the average rate in each. The corresponding squared-error for each bin was taken to be the average of squared-errors, weighted by number of observations. The error of the log-rate was taken to be $\Delta\log(r) = \Delta r/r$, where Δr is the error of the rate and r the rate.

For each simulation excavation rate curve, we calculated the average of squared differences from the observed curve, weighted by $(\Delta r)^{-2}$, in log–log, over the range of 0.5–35 h, as a measure of the quality of fit. In each refinement iteration, we used enough sampled parameter sets to display a clear trend in at least one parameter. Following each iteration we narrowed the search for those parameters that displayed a clear minimum (figure 6).

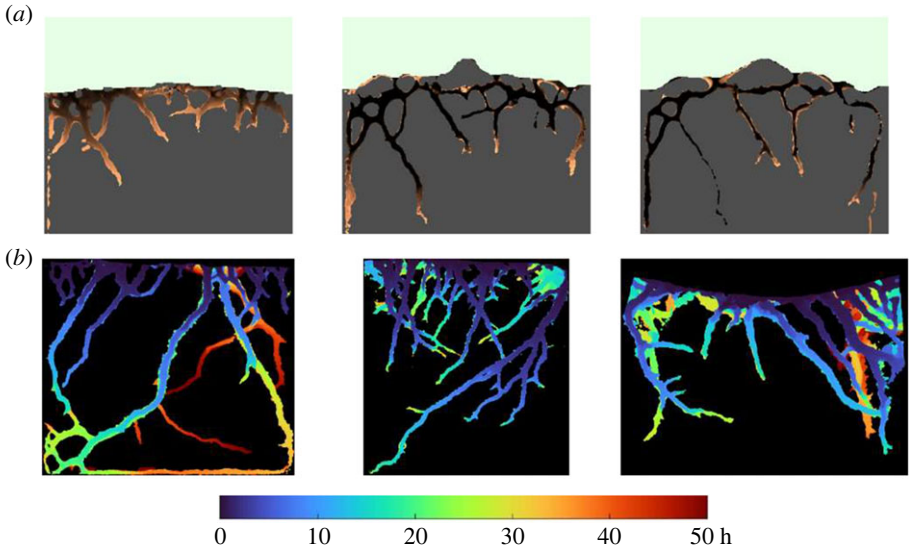

Figure 4. Flow morphology tracked by ant motion detection and colour thresholding. (*a*) Tunnel exploration over time in a single experiment. Left to right—the system, as it evolves in time slices of 3 h, over the course of the first 9 h. The substrate is tracked using colour thresholding (see Methods) and displayed in grey. Above-substrate is coloured in light green. Tunnel colour represents a spatial mapping of first-exploration time, ranging from darkest for earliest and brightest brown for latest (3 h) within the time slice. Newly detected flow indicates freshly excavated passages. Missing flow in existing tunnels may indicate a loss of interest, due to a blocked entrance or other reasons. (*b*) Tunnel formations mapped by first-exploration time, over 50 h. Left to right—three independent experiments. Unexplored areas are in black. The colour indicates first-exploration time, according to the colour map below the bottom panels.

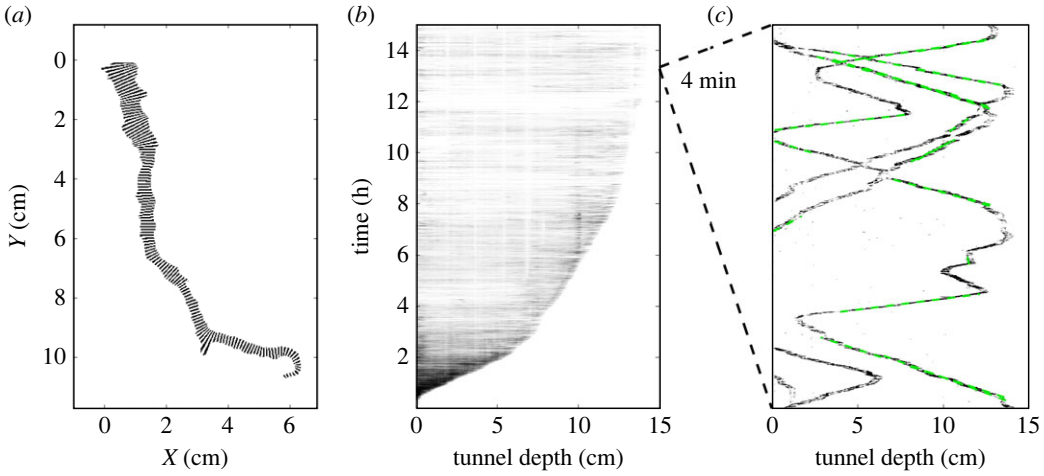

Figure 5. Analysis of space–time detection maps. (*a*) A branch-less tunnel was divided into strips of equal longitudinal distance, shown in alternating black and white strip colour. (*b*) Ant pixels were determined based on a darkness threshold, and binarized pixels were summed over every longitudinal strip, to generate a density profile over time. Ant presence was observed deeper in the tunnel as it grew through excavation. (*c*) The space–time detection maps revealed distinct tracks when observed at minutes-long windows. We used a Hough transform [58] to detect straight (i.e. constant speed) trajectories fragments (green dashed lines). From the collected line slopes we calculated an average observed ant walking speed in tunnels.

Table 1. Parameters used to calibrate the cellular-automata simulation to the experiment.

parameter	value	source
average body-length (BL)	3.95 mm	[46]
tunnel width	2.2 mm	[46]
reversal probability	0.34	[57]
average ant walking speed	0.27 BL s^{-1}	space–time analysis (figure 3)
average time spent excavating	8.5 s	visual observation
number of ant trips per cm excavated	206	visual observation

3. Results and discussion

Our overall goal was to understand the mechanisms that animal collectives use to coordinate their activities. We investigated this issue by studying patterns of tunnel excavation in fire ant societies. We combined theoretical and empirical approaches to gain insight into the possible proximate mechanisms used by fire ants to accomplish important group tasks.

3.1. Ant excavation experiments

Our first aim was to gain insight into the rate of excavation of tunnels by the ant collectives. Following the introduction of ants into the system through the entrance chamber (figure 1), ants explored the container and went through a narrow hole into the digging arena in the lower chamber, in view of the camera (see Methods). We observed that all

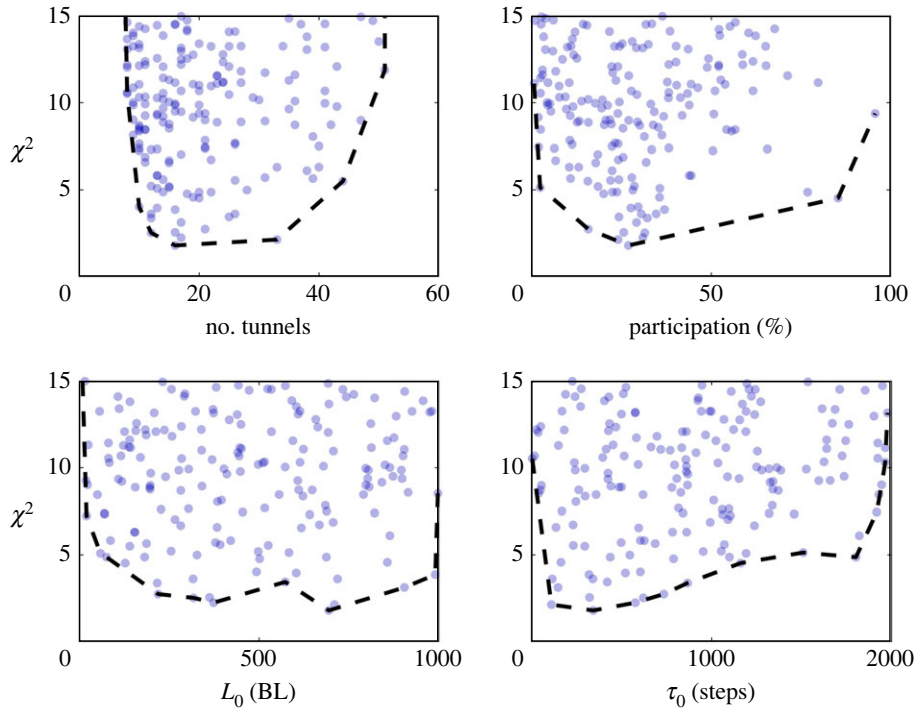

Figure 6. Least-squares (χ^2) optimization of the model fit through random parameter sampling. In each iteration, we sampled thousands of parameter variations and calculated the mean-square distance between the simulated excavation-rate trend and the experimental one. We plotted χ^2 distances versus each one of the fitted parameters (blue points), as well as an outline of their basin as a guide (black dashed line). After each such iteration we narrowed the search range for parameters with a clear single-minimum in their basin.

ants entered the lower chamber within the first hour and many engaged in excavation after a few minutes of exploration.

Within the first few hours, approximately half of the ants seemed to be excavating through multiple tunnel entrances and occasionally tunnels wide enough to accommodate three to five ants (figure 4*a*). At longer times, the tunnels grew through excavation and deposition until a few tunnel entrances remained at the top substrate interface. As the level of activity decayed, the tunnels converged to the typical width of a single BL, approximately accommodating the width of two ants [54]. Maps of first-exploration time (figure 4*b*) capture the features of tunnel formation over the course of each trial.

The area excavated over time in all the trials follows a trend of rapid increase, followed by a slower increase (figure 7*a*, non-black colours). In a few trials, additional waves of rapid excavation appear, but eventually, those too settled into a slower rate of expansion. By averaging the area excavated in all trials, this trend appears even clearer (figure 7*a*, black). Excavation (area growth) rates reveal additional subtleties when viewed over multiple timescales (figure 7*b*), where we observe three regimes: high and almost constant excavation rate, followed by a rapid decay, and then a slow decay at long times. The transition between the rapid and slow decays is quite distinct, especially considering the noise involved in experiments comprising living systems.

Previous studies of ant excavation reported similar trends [44,45,59], where the excavation rate started high or peaked, and then decreased slowly over time. Buhl *et al.* [44] model their observations empirically as a classical Verhulst logistic model. The logistic model predicts that the excavation rate should vanish exponentially in time, which is not supported by our observations (figure 7). The same model was used before by Rasse *et al.* [60], though on a much longer timescale of tens of days. Bruce *et al.* [45] empirically model the excavation rate as a power-law which predicts a t^{-2} decay in rate over time, which is also inconsistent with our observations. Neither of these previous models is derived from explicit behavioural rules, though Bruce *et al.* allude to a state of 'arousal' that may follow a disturbance or introduction into an unfamiliar system. Bruce *et al.* also make important observations about the initial excavation rate depending on group size and initial tunnel length. We will show below that these observations of arousal and length/number dependencies can be explained by a single behavioural rule that originates from the local experience of collisions.

3.2. Participation trend

To investigate the apparent regulation of excavation rate over time, we suspected two possible modulated parameters—participation level in excavation and walking speed. A previous study showed a weak decay of walking speed in time [45], not significant enough to explain our observed excavation rate. Our limited observations of walking speed did not reveal any trend in time. By contrast, we quantified the collective participation level in excavation, and discovered a distinct trend.

At all times during an experiment, a significant portion of the ants was above the substrate and not actively participating in excavation. While above the substrate, many of the non-excavating ants were found in clusters. This aggregation behaviour has been reported in previous studies, for multiple ant species [44–46,59–61]. Approximately 2–3 h into each trial, participation in excavation peaks at approximately 50% (figure 8*a*). Coincidentally, roughly at the same time, the slow excavation-rate decay begin (figure 9*a*). At later times, the

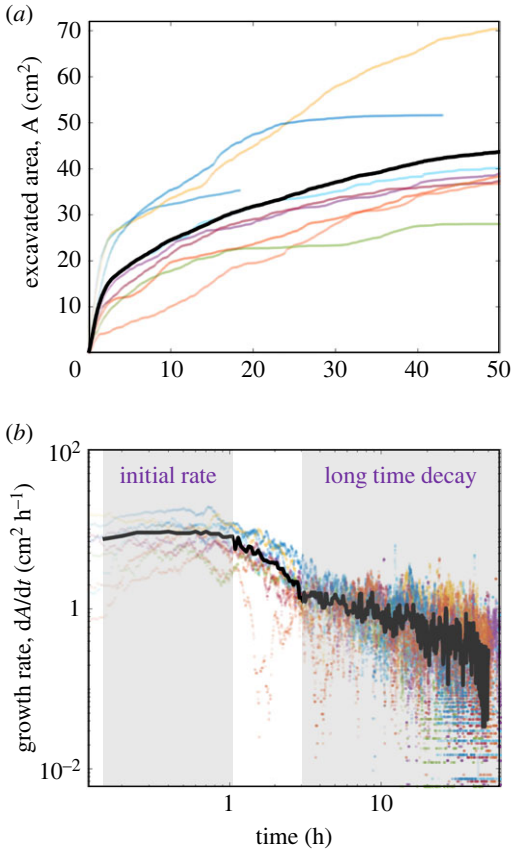

Figure 7. Excavation area dynamics for multiple trials of *S. invicta* digging. (*a*) Area excavated over time in nine independent trials (coloured points), along with their average (black line). A clear trend emerges where at the initial phase there is almost constant excavation rate, followed by a rapid decay, and at longer times a slower decay. (*b*) Area growth rate over time, with colours as in (*a*). A consistent feature of rapid excavation appears in all trials at the first few hours, followed by fast decrease in rate and a sharp transition, leading to slow decay in rate at long times.

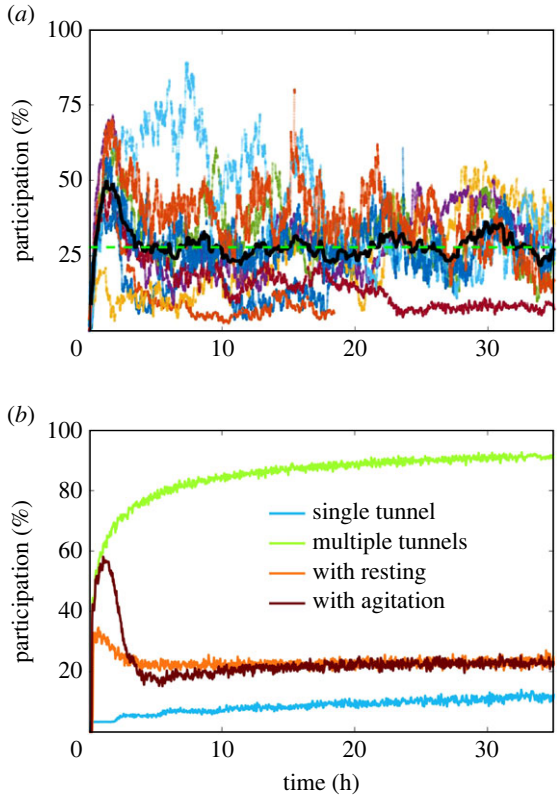

Figure 8. A varying fraction of the ant collective actively participate in excavation at any time. (*a*) Tracked ant participation in the recorded experimental trials. Each coloured line represents an individual trial. The average trend (black) peaks around 50% and later fluctuates around constant participation of approximately 27.8% (green dashed line). (*b*) CA model simulations with varying implemented features. In both a single tunnel (blue) and multiple tunnel models (green), the participation monotonically increases over time, though faster for multiple tunnels. To the multiple tunnels we added a tendency to rest and maintain a 27.8% work to rest ratio (orange). Once 'agitation' is added to the previous model on top of resting behaviour (brown), it overrides the behaviour at short tunnel lengths which manifests as a high participation peak, followed by a sharp fall.

average participation trend appears to fluctuate around a mean value of approximately 27.8% (green dashed line in figure 8*a*), calculated as the average participation between 5 and 35 h; this participation rate is consistent with previous reporting [46]. The early peak in participation correlates with the initial high excavation rate and its rapid decay, but then the rate decays further, while, surprisingly, participation remains constant.

3.3. Cellular automata behavioural model

To probe the effect of individual dynamics on participation in excavation and the emergent excavation rate, we built upon our CA model simulations in [57] (see Methods). In our previous work, we experimentally resolved the activity of ants at the individual level, while excavating a single tunnel, and consistently observed a highly unequal workload distribution among excavating ants [57]. In corresponding CA simulations, individuals were initialized to have a preset equal or unequal tendency to enter tunnels; an unequal tendency to enter the tunnels was crucial for avoiding long-duration clogs and maintaining optimal traffic flow conditions. Recently, we reported on the implementation of reinforcement rules in a collective of excavating robots that results in unequal workload distribution and improved group performance [51]. In fire ants, it was reported that groups adapt to the removal of the most active workers by upregulating the activity of others [57], though we do not know what mechanism they use to accomplish that.

The model we developed (below) generates unequal workload at any given moment, but the turnover between ants equalizes the workload quickly, compared with previous observations of persistent inequality over 12 h [57]. Notably, in [57] (electronic supplementary material), some turnover in levels of activity was also observed. This inconsistency can be regarded as a level of abstraction, where we capture the collective level of activity but not the workload distribution. The collective rate of excavation, which is of interest here, scales as the number of actively excavating ants, or mean participation level, at low ant densities. Workload inequality—the individual deviations from the mean participation—is a second-order effect which we do not consider in this work.

First, we compared unmodified CA model simulations (figure 3*a*) [57], originally developed to reproduce excavation in a single tunnel, to the observed experimental trend and found the excavation rate trend produced by the CA model was far below that actually observed (figure 9). Expanding the CA model to include multiple independent tunnels sharing an ant reservoir results in a higher excavation rate, where a model with 10 tunnels captures the experimental long-time

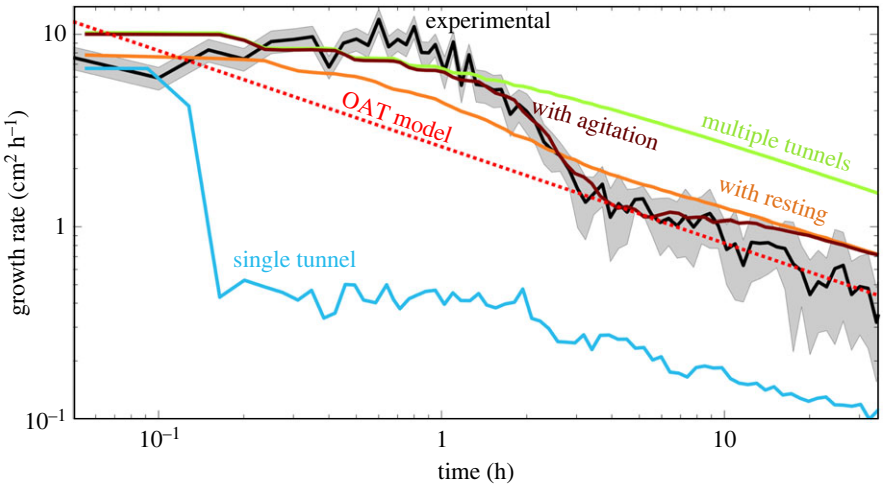

Figure 9. Experimental and computer-simulated excavation rate over time. CA model simulation fit to the excavation rate (brown line) over the experimental average (black line) and its standard deviation (shaded). The fit was generated by a model including a mean free path dependent 'agitation' override. The same model was also run, for reference, without 'agitation' (orange line), also without resting behaviour (green line), and finally also without multiple tunnels (blue line, multiplied by 10). Both models, as well as the experimental trend, are consistent with a one-at-a-time (OAT) like $t^{-1/2}$ asymptotic behaviour (red dotted line, scaled to match experiment at long times).

average trend (figure 9). Interestingly, both the unmodified and multi-tunnel CA models already capture the experimental long-time decay trend (figure 9). This result suggests that the slow decay is an inevitable result of excavation in an elongating tunnel.

Our multi-tunnel CA model still did not capture the early time rate trend that coincided with regulated participation. Moreover, the participation of ants in excavation saturates at 100% in the CA model, regardless of number of tunnels and in contrast with the experiment (figure 8). We thus posit that a stable and low participation in excavation requires a self-limiting process.

We observed in experiments that most of the ants above the substrate aggregated together in clusters of inactive individuals; this inactivity invoked the possibility of a resting behaviour. Therefore, we implemented a self-limiting process in the CA simulations, maintaining a fixed work-to-rest ratio R. We define a work–rest imbalance as $t_{\mathrm{imbalance}} = t_{\mathrm{work}} - R \cdot t_{\mathrm{rest}}$, where t_{work} (t_{rest}) is the time an ant spent working (resting). An ant is set to go excavate with probability $P_{\mathrm{go}} = \exp(-t_{\mathrm{imbalance}}/\tau_{\mathrm{tolerance}})$, where $\tau_{\mathrm{tolerance}}$ is a timescale for the tolerance of a work-to-rest imbalance. Inclusion of this parameter indeed results in a low and stable participation in the CA simulation at long times (figure 8, green line), and an excavation-rate trend consistent with most of the experimentally observed curve (figure 9, green line). This model can also accommodate previous observations of an unequal workload distribution among ants [57] by replacing the work–rest imbalance ratio with a distribution.

While the CA model with regulated participation is consistent with the observed rate, it does not capture the steepness of the observed rate decay at early times (figure 9, up to third hour). This mismatch implied an additional mechanism is at play that maintains high excavation rate at early times and generates a sharp transition to the long-time behaviour.

We propose that the ants are willing to delay rest when excavating a fresh system of tunnels, until they detect the tunnels are large enough, at which point they revert to a nominal behaviour pattern. Such a mechanism implies that the insects become agitated without shelter, and relax into nominal behaviour when sheltered, consistent with the concept of 'arousal' described before [45].

We, therefore, amended our CA simulations to include a digging probability with an 'agitation' override: $p = (1-\alpha)\cdot p_{\mathrm{go}} + \alpha$, where $\alpha \in [0,1]$ is an override parameter. Setting $\alpha = 1$ completely overrides the effect of a work–rest imbalance on the decision to go dig excavate. But what exactly do the ants detect, and does communication play a role?

Here, we define communication broadly as when one individual receives information from another, and this information affects the future actions of the focal individual. A reasonable type of information that can be obtained by an individual ant is its collision with other individuals and its surroundings. These collisions are accounted for through the success rate of moving forward, the inverse of which is essentially an estimate for mean free path. We, therefore, set α to be $\alpha = e^{-l/L_0}$, where l^{-1} is a move success-rate estimator and L_0 is a length constant. By defining an ant's response this way, we obtain a unified view of collisions with other ants, as well as with the end of the tunnel.

The expected mean free path in any single tunnel is L/f, where L is the tunnel length and f is the (expected) number of failed moves, cause by the tunnel end and cells occupied by two ants. A single ant in a tunnel will experience $f = 1$ failed moves, and will, therefore, estimate $l \approx L$. In a mean-field calculation, f is expected to be $L \cdot P(\text{two ants in one cell}) \propto L \cdot (N/L)^2$, where N is the number of ants in the tunnel, which would result in $l \propto L^2/N^2$. This mechanism effectively has a quadratic sensitivity to the density of ants in the tunnels. In practice, our move success-rate estimator (l^{-1}) implementation uses an exponential moving average with a memory time constant of $2L_0$ to avoid infinitely long memory.

The result of this length-dependent relaxation mechanism is a higher tendency for the simulated ants to excavate at short tunnel lengths, overriding the steady-state work–rest behaviour. As the length of a tunnel increases, the participation of ants in excavation relaxes to its steady-state value.

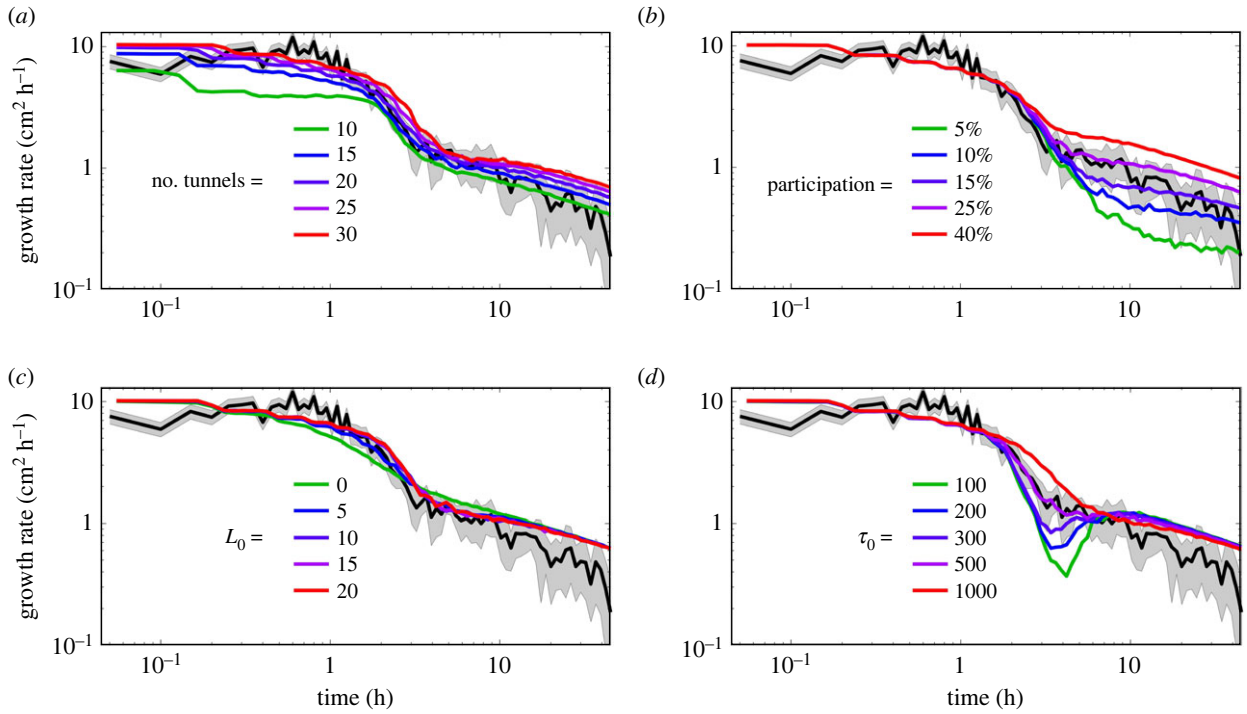

Figure 10. Parameter variation effects on modelled excavation rate. The best-fit model parameters were perturbed one at a time, around the best-fit value, while keeping the rest fixed. The resulting variations in computed excavation rate (averaged over 11 runs) are depicted in coloured lines, overlaying the experimental average (black line) and its standard deviation (shaded). (*a*) Varying number of tunnels. (*b*) Varying steady-state ant participation rate in excavation. (*c*) Varying 'agitation' relaxation length L_0. (*d*) Varying work-to-rest imbalance tolerance τ_0.

As noted above, the mean free path estimator is highly density dependent through three+ body collisions, since there is no penalty (delay) for two-body collisions in the simulation. At tunnel lengths reaching the designated relaxation length L_0, some ants decide to rest, which further reduces density in the tunnel, and as a result a cascade of relaxation into the steady-state behaviour occurs. This cascade gives rise to a sharp transition in excavation rate, closely matching the observed experimental trend (figure 9, blue line).

Our developed CA model captures the subtleties of observed collective ant excavation behaviour, and its success suggests a behavioural mechanism employed by the individuals. Parameter variation around the best-fit solution demonstrates the observed features associated with each parameter, and in particular—that the relaxation length (L_0) modulates the steepness of the transition between early and long-time stages (figure 10). In figure 10*a*, we observe a scaling of the curve for more than 15 tunnels, but a qualitatively different trend at early times for 10 tunnels. This qualitative change highlights the necessity of many tunnels to alleviate traffic congestion and achieve the high excavation rate at early times. Branching is prevalent in the experimental trials at early times (figure 4), and probably increases the effective number of tunnels needed for the CA model to match. In figure 10*b*, we show that the steady-state participation level does not affect early times, as a result of the 'agitation' override. The overall response to varying L_0 in figure 10*c* is nonlinear and saturates at a value of 10 due to the nonlinear dependence of the mean free path in the density of ants in the tunnel, and the mechanism of its estimation by the modelled ants.

It is worth noting that our 'agitation' override captures previous concepts of 'arousal' and initial tunnel-length effect. The model also predicts faster relaxation with fewer ants, as fewer ants would result in fewer collisions for the same number of tunnels. Whether they would relax faster or not depends on the actual number of tunnels they generate, which may be affected by the width of the arena.

In this work, we introduced a resting mechanism employed homogeneously by all simulated ants, which results in a nearly equal workload distribution (data not shown). This is in contrast with previous findings of unequal participation in work and the potential rules leading up to it [51,57]. Our focus in this work was on emergent global regulation, rather than emergent workload distributions. The CA model here essentially captures the same global inequality as low participation rates at any moment, but the work is spread among all individuals. The same can be implemented with an unequal workload, by setting target work-to-rest ratios heterogeneously among the simulated individuals.

3.4. The one-at-a-time model

We turn our attention back to the seeming inevitability of the long-time excavation rate decay, which appears in experiment as well as in all of our CA model variation. Ants working inside a narrow tunnel can be considered as one-dimensional asymmetric exclusion processes with few lanes [57,62,63]. Let us consider an unregulated excavation-rate behaviour with a single ant, digging in a single tunnel. This ant performs a consistent walking and excavation procedure over time, going back and forth, digging at the tip of the tunnel and depositing dug pellets at the entrance (figure 11). We call this scenario the one-at-a-time (OAT) model, which we found experimental support for [57].

In this scenario, each digging cycle takes a time of $(2L/v) + \tau_{dd}$, where L is the tunnel length, v is the ant moving speed and τ_{dd} is the time it takes to manipulate the substrate while digging and depositing at either end of the

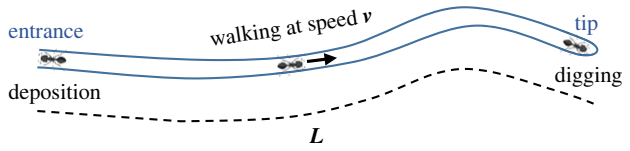

Figure 11. Illustration of the one-at-a-time model. A single ant walks back and forth from the entrance of the tunnel to the tip. It digs at the tip and deposits the dug pellets at the entrance. The time for digging and deposition τ_{dd} is assumed to be constant. In between the entrance and the tip, the ant walks at speed v across the length of the tunnel L that extends over time.

tunnel. The average excavation rate for K non-interacting ants will then be $dL/dt = K/(2L/v + \tau_{dd})$.

The corresponding tunnel growth follows the length–time relationship: $L(t) = 1/2\left(-v\tau_{dd} + \sqrt{v^2\tau_{dd}^2 + 4Kvt}\right)$, where the initial condition is set to $L(t=0) = 0$. By taking the long-time limit $t \to \infty$ we see that in the OAT model, the tunnel length asymptotically grows as $t^{1/2}$, and the corresponding tunnel excavation rate follows $1/L \propto t^{-1/2}$ at long tunnel length or late time. Though this was derived for an ideal situation, it clearly extends to any scenario with a constant number of participating ants and negligible time spent on collisions or any activity other than walking and manipulating substrate. Remarkably, this derived long-time rate trend agrees with both experiments and the CA model (figure 9, red dashed line). We posit that our observation of an OAT-like trend at long times (figure 9) is most likely a consequence of negligible interactions between active ants and a stable participation level, which our CA model generates.

4. Summary and conclusion

The goal of this study was to understand the dynamics of excavation behaviour by collectives of ants as model social insects which regularly confront crowded traffic conditions in a confined space. We performed ant excavation experiments in a quasi-two-dimensional system and observed a pattern of excavation-rate modulation [44,45,60]. Our experimental excavation rate trend reveals signs of regulation across timescales, including a high and constant initial rate, a fast decay, and a slow decay at long timescales (figure 7).

We developed a detailed, behavioural, CA model, carefully motivated and with most of its parameters derived from independent observations. Our model captures the experimental excavation rate trend very well across timescales, and suggests ants modulate their participation in excavation based on their recent history of collisions. Crucially, this modulation, which we refer to as an 'agitation override', addresses observed effects of both initial tunnel length and ant group size, and serves as a mechanistic description of the concept of 'arousal' which is referred to in [45].

Previous studies employed empirical models such as a logistic model or a power-law to describe their excavation rate observations without being clearly motivated by behavioural rules at the individual level [44,45,60]. We derive a quantitative fit, by introducing resting behaviour, which can be overridden in a state of agitation. Both the regulation of work–rest and agitation is done by each individual in our model. Agitation is determined from length estimates based on collisions with others, as well as with the end of the tunnel. Moreover, we showed that an idealized 'one-at-a-time' model, derived by considering the fundamental timescales in the system, predicts that the excavation rate at long times should decay like $t^{-1/2}$. This prediction fits our experimental observation and expectations at long timescales surprisingly well.

Our models do not include many aspects of the tunnel system, such as width variations, formation of branches, and unequal investment in the excavation of each tunnel. Despite that, the success of CA models in this (figure 9) and previous work [57] is promising, and could be extended to include other behaviours and additional details. We propose that CA models with similar rules might be applied to other social insects that perform tasks in crowded confined environments.

5. Permission to re-use and copyright

Data accessibility. Relevant data and code are available at Figshare: https://doi.org/10.6084/m9.figshare.22649689.v1 [64].

Authors' contributions. R.A.: data curation, formal analysis, investigation, methodology, software, validation, visualization, writing—original draft, writing—review and editing; K.O.A.: conceptualization, investigation, methodology, writing—original draft; C.J.D.: conceptualization, investigation, methodology, writing—original draft; H-S.K.: conceptualization, formal analysis, investigation; M.D.B.: conceptualization, formal analysis, methodology; M.A.D.G.: conceptualization, funding acquisition, investigation, methodology, project administration, supervision, writing—original draft, writing—review and editing; D.I.G.: funding acquisition, methodology, project administration, supervision, validation, writing—original draft, writing—review and editing.

All authors gave final approval for publication and agreed to be held accountable for the work performed therein.

Conflict of interest declaration. We declare we have no competing interests.

Funding. Funding for this research provided by ARO MURI award W911NF-19-1-023, NSF Grant PHY-1205878, NSF Grant IOS-2019799 to M.A.D.G. and D.I.G. and NSF Grant DMR-1725065 to M.D.B.

References

1. Sumpter DJ. 2005 The principles of collective animal behaviour. *Phil. Trans. R. Soc. B* **361**, 5–22. (doi:10.1098/rstb.2005.1733)
2. Vicsek T, Zafeiris A. 2012 Collective motion. *Phys. Rep.* **517**, 71–140. (doi:10.1016/j.physrep.2012.03.004)
3. Couzin ID. 2009 Collective cognition in animal groups. *Trends Cogn. Sci.* **13**, 36–43. (doi:10.1016/j.tics.2008.10.002)
4. Nadell CD, Bucci V, Drescher K, Levin SA, Bassler BL, Xavier JB. 2013 Cutting through the complexity of cell collectives. *Proc. R. Soc. B* **280**, 20122770. (doi:10.1098/rspb.2012.2770)
5. Detrain C, Deneubourg J-L. 2006 Self-organized structures in a superorganism: do ants 'behave' like

molecules? *Phys. Life Rev.* **3**, 162–187. (doi:10.1016/j.plrev.2006.07.001)

6. Feinerman O, Korman A, Levine JD, Kronauer DJC, Dickinson MH. 2017 Individual versus collective cognition in social insects. *J. Exp. Biol.* **220**, 73–82. (doi:10.1242/jeb.143891)
7. Camazine S, Deneubourg J-L, Franks NR, Sneyd J, Theraula G, Bonabeau E. 2003 *Self-organization in biological systems*. Princeton, NJ: Princeton University Press.
8. Saha T, Galic M. 2018 Self-organization across scales: from molecules to organisms. *Phil. Trans. R. Soc. B* **373**, 20170113. (doi:10.1098/RSTB.2017.0113)
9. Queller DC, Strassmann JE. 1998 Kin selection and social insects. *Bioscience* **48**, 165–175. (doi:10.2307/1313262)
10. Wilson EO. 1971 *The insect societies*. Cambridge, MA: Harvard University Press.
11. Strassmann JE, Queller DC. 2007 Insect societies as divided organisms: the complexities of purpose and cross-purpose. *Proc. Natl Acad. Sci. USA* **104**, 8619–8626. (doi:10.1073/pnas.0701285104)
12. Hansell M. 2005 *Animal architecture*. Oxford, UK: Oxford University Press.
13. Pinter-Wollman N. 2015 Nest architecture shapes the collective behaviour of harvester ants. *Biol. Lett.* **11**, 20150695. (doi:10.1098/rsbl.2015.0695)
14. Cassill D, Tschinkel WR, Vinson SB. 2002 Nest complexity, group size and brood rearing in the fire ant, *Solenopsis invicta*. *Insectes Soc.* **49**, 158–163. (doi:10.1007/s00040-002-8296-9)
15. Cruz MG, Boster FJ, Rodriguez JI. 1997 The impact of group size and proportion of shared information on the exchange and integration of information in groups. *Commun. Res.* **24**, 291–313. (doi:10.1177/009365097024003004)
16. Turner JS. 2000 *The extended organism: the physiology of animal-built structures*. Cambridge, MA: Harvard University Press.
17. Pinter-Wollman N, Fiore SM, Theraulaz G. 2017 The impact of architecture on collective behaviour. *Nat. Ecol. Evol.* **1**, 0111. (doi:10.1038/s41559-017-0111)
18. Pinter-Wollman N, Penn A, Theraulaz G, Fiore SM. 2018 Interdisciplinary approaches for uncovering the impacts of architecture on collective behaviour. *Phil. Trans. R. Soc. B* **373**, 20170232. (doi:10.1098/rstb.2017.0232)
19. Tschinkel WR. 2004 The nest architecture of the Florida harvester ant, *Pogonomyrmex badius*. *J. Insect Sci.* **4**, 21. (doi:10.1093/jis/4.1.21)
20. Bollazzi M, Roces F. 2007 To build or not to build: circulating dry air organizes collective building for climate control in the leaf-cutting ant *Acromyrmex ambiguus*. *Anim. Behav.* **74**, 1349–1355. (doi:10.1016/j.anbehav.2007.02.021)
21. Jones JC, Oldroyd BP. 2007 Nest thermoregulation in social insects. *Adv. Insect Physiol.* **33**, 153–191. (doi:10.1016/S0065-2806(06)33003-2)
22. Mikheyev AS, Tschinkel WR. 2004 Nest architecture of the ant *Formica pallidefulva*: structure, costs and rules of excavation. *Insectes Soc.* **51**, 30–36. (doi:10.1007/s00040-003-0703-3)
23. Perna A, Jost C, Couturier E, Valverde S, Douady S, Theraulaz G. 2008 The structure of gallery networks in the nests of termite *Cubitermes* spp. revealed by X-ray tomography. *Naturwissenschaften* **95**, 877–884. (doi:10.1007/s00114-008-0388-6)
24. Diehl-Fleig E, Diehl E. 2007 Nest architecture and colony size of the fungus-growing ant *Mycetophylax simplex* Emery, 1888 (Formicidae, Attini). *Insectes Soc.* **54**, 242–247. (doi:10.1007/s00040-007-0936-7)
25. Forti LC, Camargo RS, Fujihara RT, Lopes JFS. 2007 The nest architecture of the ant, *Pheidole oxyops* Forel, 1908 (Hymenoptera: Formicidae). *Insect Sci.* **14**, 437–442. (doi:10.1111/j.1744-7917.2007.00171.x)
26. Buhl J, Gautrais J, Sole RV, Kuntz P, Valverde S, Deneubourg JL, Theraulaz G. 2004 Efficiency and robustness in ant networks of galleries. *Eur. Phys. J. B* **42**, 123–129. (doi:10.1140/epjb/e2004-00364-9)
27. Buhl J, Gautrais J, Deneubourg JL, Theraulaz G. 2004 Nest excavation in ants: group size effects on the size and structure of tunneling networks *Naturwissenschaften* **91**, 602–606. (doi:10.1007/s00114-004-0577-x)
28. Buhl J, Gautrais J, Deneubourg JL, Kuntz P, Theraulaz G. 2006 The growth and form of tunnelling networks in ants. *J. Theor. Biol.* **243**, 287–298. (doi:10.1016/j.jtbi.2006.06.018)
29. Lee SH, Bardunias P, Su NY. 2008 Rounding a corner of a bent termite tunnel and tunnel traffic efficiency. *Behav. Processes* **77**, 135–138. (doi:10.1016/j.beproc.2007.06.012)
30. Strogatz SH. 2001 Exploring complex networks. *Nature* **410**, 268–276. (doi:10.1038/35065725)
31. Invernizzi E, Ruxton GD. 2019 Deconstructing collective building in social insects: implications for ecological adaptation and evolution. *Insectes Soc.* **66**, 507–518. (doi:10.1007/s00040-019-00719-7)
32. Gordon DM. 2019 The ecology of collective behavior in ants. *Annu. Rev. Entomol.* **64**, 35–50. (doi:10.1146/annurev-ento-011118-111923)
33. Wenzel JW. 1991 Evolution of nest architecture. In *The social biology of wasps*. Ithaca, NY: Comstock publishing associates.
34. Theraulaz G, Bonabeau E, Deneubourg J-L. 1998 The origin of nest complexity in social insects. *Complexity* **3**, 15–25. (doi:10.1002/(SICI)1099-0526(199807/08)3:6<15::AID-CPLX3>3.0.CO;2-V)
35. Theraulaz G, Gautrais J, Camazine S, Deneubourg JL. 2003 The formation of spatial patterns in social insects: from simple behaviours to complex structures. *Phil. Tran. R. Soc. Lond. A* **361**, 1263–1282. (doi:10.1098/rsta.2003.1198)
36. Perna A, Theraulaz G. 2017 When social behaviour is moulded in clay: on growth and form of social insect nests. *J. Exp. Biol.* **220**, 83–91. (eds JD Levine, DJC Kronauer, MH Dickinson). (doi:10.1242/jeb.143347)
37. Korb J. 2003 Thermoregulation and ventilation of termite mounds. *Naturwissenschaften* **90**, 212–219. (doi:10.1007/s00114-002-0401-4)
38. Fewell JH. 2003 Social insect networks. *Science* **301**, 1867–1870. (doi:10.1126/science.1088945)
39. Bonabeau E, Theraulaz G, Deneubourg J, Franks NR, Rafelsberger O, Joly J, Blanco S. 1998 A model for the emergence of pillars, walls and royal chambers in termite nests. *Phil. Trans. R. Soc. Lond. B* **353**, 1561–1576. (doi:10.1098/rstb.1998.0310)
40. Bardunias PM, Su N-Y. 2010 Queue size determines the width of tunnels in the Formosan subterranean termite (Isoptera: Rhinotermitidae). *J. Insect Behav.* **23**, 189–204. (doi:10.1007/s10905-010-9206-z)
41. Khuong A, Gautrais J, Perna A, Sbaï C, Combe M, Kuntz P, Jost C, Theraulaz G. 2016 Stigmergic construction and topochemical information shape ant nest architecture. *Proc. Natl Acad. Sci. USA* **113**, 1303–1308. (doi:10.1073/pnas.1509829113)
42. Kolay S, Boulay R, D'Ettorre P. 2020 Regulation of ant foraging: a review of the role of information use and personality. *Front. Psychol.* **11**, 734. (doi:10.3389/fpsyg.2020.00734)
43. Sempo G, Detrain C. 2010 Social task regulation in the dimorphic ant, *Pheidole pallidula*: the influence of caste ratio. *J. Insect Sci.* **10**, 1–16. (doi:10.1673/031.010.0301)
44. Buhl J, Deneubourg JL, Grimal A, Theraulaz G. 2005 Self-organized digging activity in ant colonies. *Behav. Ecol. Sociobiol.* **58**, 9–17. (doi:10.1007/s00265-004-0906-2)
45. Bruce AI, Pérez-Escudero A, Czaczkes TJ, Burd M. 2019 The digging dynamics of ant tunnels: movement, encounters, and nest space. *Insectes Soc.* **66**, 119–127. (doi:10.1007/s00040-018-0657-0)
46. Gravish N, Garcia M, Mazouchova N, Levy L, Umbanhowar PB, Goodisman MAD, Goldman DI. 2012 Effects of worker size on the dynamics of fire ant tunnel construction. *J. R. Soc. Interface* **9**, 3312–3322. (doi:10.1098/rsif.2012.0423)
47. Srinivasan B. 2021 A guide to the Michaelis–Menten equation: steady state and beyond. *FEBS J.* **289**, 6086–6098. (doi:10.1111/febs.16124)
48. Hölldobler B, Wilson EO. 1990 *The ants*. Heidelberg, Germany: Springer Berlin.
49. Czaczkes TJ, Grüter C, Ratnieks FL. 2015 Trail pheromones: an integrative view of their role in social insect colony organization. *Annu. Rev. Entomol.* **60**, 581–599. (doi:10.1146/annurev-ento-010814-020627)
50. Li S, Dutta B, Cannon S, Daymude JJ, Avinery R, Aydin E, Richa AW, Goldman DI, Randall D. 2021 Programming active cohesive granular matter with mechanically induced phase changes. *Sci. Adv.* **7**, 8494–8517. (doi:10.1126/sciadv.abe8494)
51. Aina KO, Avinery R, Kuan H-S, Betterton MD, Goodisman MAD, Goldman DI. 2022 Toward task capable active matter: learning to avoid clogging in confined collectives via collisions. *Front. Phys.* **10**, 1–13. (doi:10.3389/fphy.2022.735667)
52. Tschinkel WR. 2006 *The fire ants*. Cambridge, MA: Harvard University Press.
53. Gravish N, Gold G, Zangwill A, Goodisman MAD, Goldman DI. 2015 Glass-like dynamics in confined and congested ant traffic. *Soft Matter* **11**, 6552–6561. (doi:10.1039/C5SM00693G)

54. Gravish N, Monaenkova D, Goodisman MA, Goldman DI. 2013 Climbing, falling, and jamming during ant locomotion in confined environments. *Proc. Natl Acad. Sci. USA* **110**, 9746–9751. (doi:10.1073/pnas.1302428110)
55. Jouvenaz DP, Allen GE, Banks WA, Wojcik DP. 1977 A survey for pathogens of fire ants, *Solenopsis* spp., in the Southeastern United States. *Fla. Entomol.* **60**, 275. (doi:10.2307/3493922)
56. Monaenkova D, Gravish N, Rodriguez G, Kutner R, Goodisman MA, Goldman DI. 2015 Behavioral and mechanical determinants of collective subsurface nest excavation. *J. Exp. Biol.* **218**, 1 295–1 305. (doi:10.1242/jeb.113795)
57. Aguilar J, Monaenkova D, Linevich V, Savoie W, Dutta B, Kuan H-S, Betterton MD, Goodisman MAD, Goldman DI. 2018 Collective clog control: optimizing traffic flow in confined biological and robophysical excavation. *Science* **361**, 672–677. (doi:10.1126/science.aan3891)
58. Duda RO, Hart PE. 1972 Use of the Hough transformation to detect lines and curves in pictures. *Commun. ACM* **15**, 11–15. (doi:10.1145/361237.361242)
59. Deneubourg JL, Lioni A, Detrain C. 2002 Dynamics of aggregation and emergence of cooperation. *Biol. Bull.* **202**, 262–267. (doi:10.2307/1543477)
60. Rasse P, Deneubourg JL. 2001 Dynamics of nest excavation and nest size regulation of *Lasius niger* (Hymenoptera: Formicidae). *J. Insect Behav.* **14**, 433–449. (doi:10.1023/A:1011163804217)
61. Jeanson R, Deneubourg JL, Grimal A, Theraulaz G. 2004 Modulation of individual behavior and collective decisionmaking during aggregation site selection by the ant *Messor barbarus*. *Behav. Ecol. Sociobiol.* **55**, 388–394 . (doi:10.1007/s00265-003-0716-y)
62. Kuan H-S, Betterton MD. 2016 Phase-plane analysis of the totally asymmetric simple exclusion process with binding kinetics and switching between antiparallel lanes. *Phys. Rev. E* **94**, 022419. (doi:10.1103/PhysRevE.94.022419)
63. Melbinger A, Reichenbach T, Franosch T, Frey E. 2011 Driven transport on parallel lanes with particle exclusion and obstruction. *Phys. Rev. E* **83**, 031923. (doi:10.1103/PhysRevE.83.031923)
64. Avinery R, Aina KO, Dyson CJ, Kuan H-S, Betterton MD, Goodisman M, Goldman DI. 2023 Labeled tracking videos and scripts. Figshare. (doi:10.6084/m9.figshare.22649689.v1)